METHODS

Theoretical Evaporite Calculations

Seawater evaporation simulations were run with the EQL/EVP program (Risacher and Clement, 2001). This program calculates solution composition and mineral precipitates throughout evaporation of the parent solution. Evaporation occurs with equilibrium between crystals and brine (i.e. crystals may redissolve during the simulation if thermodynamic mineral stabilities change). With modern SO_4-rich seawater, gypsum begins to precipitate at a concentration factor (*fc*, defined as the initial volume of seawater divided by volume of brine at time *t*) of 3.4, and halite begins to precipitate at *fc* = 11.0. Since initial SO_4 is in excess of initial Ca, Ca becomes depleted during this interval while the concentration of SO_4 continues to rise in the brine. At halite saturation, 92% of the initial Ca has been removed, the vast majority of it during the sulfate facies. Rayleigh distillation of the Ca occurs such that *R* (the ratio of $^{44}Ca/^{40}Ca$) in the fluid follows the relationship $f\_Ca^{(\alpha-1)}$, where *f_Ca* is the fraction of Ca remaining in the fluid, and α is the fractionation factor $R_{crystal}/R_{fluid}$. With a fractionation of -0.95‰ (i.e. α = 0.99905) during calcium sulfate precipitation (Hensley, 2006), Rayleigh distillation would generate brines and crystals enriched by 2.2‰ at the point of halite saturation (Fig. DR2).

For artificial Ca-rich seawater modeled after Silurian fluid inclusion analyses (Brennan and Lowenstein, 2002), the EQL/EVP program indicates initiation of gypsum precipitation at *fc* = 2.9 and halite precipitation at *fc* = 10.5. In contrast to the simulation of modern seawater, SO_4 becomes depleted while excess Ca remains in the brine. At halite saturation, only 38% of the Ca has been removed, leading to an isotopic enrichment of less than 0.5‰ (Fig. DR2).

Beaker Experiments

The recipe of Kester et al. (Kester et al., 1967) was used to generate 1 kg of modern seawater by mixing NaCl, Na_2SO_4, KCl, $NaHCO_3$, KBr, H_3BO_3, NaF, $MgCl_2 \cdot 6H_2O$, $CaCl_2 \cdot 2H_2O$, and $SrCl_2 \cdot 6H_2O$ salts and equilibrating the solution with atmospheric CO_2. A modification of the recipe was used to create 1 kg of "Silurian" seawater, following the results of fluid-inclusion analyses (Brennan and Lowenstein, 2002). These solutions were evaporated in glass beakers inside a fume hood at room temperature (25 °C).

Small aliquots (100-150 μL) of the fluid were sampled periodically along with crystal rafts that grew on the brine surface. Crystals were carefully patted dry to absorb all extra fluid and prevent additional salt precipitation from the brine wetting the samples. After sampling, the beakers were stirred such that all remaining crystals on the surface sank to the bottom. This

ensured that future crystal rafts that were observed floating on the surface had grown since the latest sampling event and would not incorporate precipitates from a previous growth interval.

The large evaporative enrichments observed in fluid and crystal $\delta^{44/40}$Ca are greater than those observed in previous experiments (Hensley, 2006), where approximately 60% of the predicted isotopic range was measured. Those experiments were carried out over 28 hours, and additional kinetic effects may have become important. The experiments in this study were carried out over approximately three weeks to allow for slower mineral precipitation.

Concentration Analyses

Major ion concentrations were determined on a Thermo Dionex 5000+ ion chromatography (IC) system. This automated system runs samples through an in-line CS16 cation exchange column which separates various cations and measures peak intensities of individual species. Seawater standards were run at various dilutions to establish linear calibrations for Na, K, and Ca. Since K is not removed in any major evaporite phase during the beaker experiments (late-stage potash evaporite facies were not reached), Ca/K ratios were used to establish the fraction of Ca remaining in solution throughout the experiments.

Sample Preparation

Geological samples were powdered with a drill press and analyzed by X-ray diffractometry (XRD) at the Imaging and Analysis Center at PRISM (Princeton Institute for the Science and Technology of Materials). A Bruker D8 Discover XRD instrument was used to determine sample mineralogy, using a Cu-Kα X-ray source at 40 mA and 40 kV, scanning from 20-50° with a step size of 0.02° and 0.2 sec/step. Samples were mounted on a glass slide and wrapped with low-density polyethylene plastic wrap. Diagnostic peaks used for mineral identification include $2\theta = 26.5°$ for anhydrite, 29.0° for gypsum, 29.3° for calcite, and 30.8° for dolomite. Following XRD analysis, small amounts of powder (0.5-1 mg) were sampled and dissolved in 2N HCl for ion chromatography. Other samples (fluids and crystals from evaporation experiments) were directly dissolved/diluted in 2N HCl.

Dissolved samples were prepared for Ca-isotope analysis with two-stage column chemistry. Samples were loaded onto 1.6 mL AG50W-X12 resin beds in 0.5 mL 2N HCl, then eluted with 11.5 mL additional 2N HCl. The Ca and Sr from the sample was then collected by eluting 12 mL 6N HCl through the column. When this fraction dried, it was then redissolved in 0.2 mL 3N HNO_3 and loaded onto a 150 µL Sr-resin bed, with immediate collection of the Ca fraction by eluting 600 µL 3N HNO_3 while Sr is retained in the resin. This fraction was then dried, treated with concentrated HNO_3, then re-dried and redissolved in 2% HNO_3. Samples were diluted to a concentration of 2ppm for Ca-isotope analysis.

Isotopic Analysis

Ca-isotope measurements were performed on a Thermo Neptune Plus at the Princeton University Department of Geosciences. Analyses were performed in medium resolution (MR) with an ESI Apex-IR sample introduction/desolvation system, with the ^{42}Ca beam measured on the low-mass shoulder of the peak to avoid the interference from ArHH. Samples of 2ppm total Ca were used, with samples and standards diluted carefully to the same concentration (within 5%) to ensure equable contributions from any Ar-based interferences and avoid concentration-dependent isotope effects. Beam intensities were measured for ^{42}Ca, ^{43}Ca, and ^{44}Ca, as well as for mass 43.5, which records double-charged ^{88}Sr and can be used to correct for Sr interferences on Ca beams. Standard-bracketed ratios of $^{44}Ca/^{42}Ca$ are used to calculate $\delta^{44/42}Ca$ against an internal standard (a single-element ICP Ca standard) which is offset from seawater by -0.45‰. Values are then converted to $\delta^{44/40}Ca$ and reported relative to seawater. Plots of $\delta^{44/43}Ca$ to $\delta^{44/42}Ca$ ensure mass-dependent fractionation and serve as a quality-control check. Long-term external reproducibility on $\delta^{44/40}Ca$ is 0.12‰, based on replicate measurements of standards which are treated as samples and undergo the entire ion chromatography procedure.

Determination of Marine Origin of Evaporites

The dominant cation chemistry of the evaporites analyzed must have a marine origin for this Ca-isotope method to be diagnostic of original seawater chemistry. For the Silurian Salina Group and the Permian Castile Formation, Sr-isotope analyses that match the global seawater $^{87}Sr/^{86}Sr$ curve confirm their marine origins (Brookins, 1988; Das et al., 1990; Kirkland et al., 2000). The Cretaceous Muribeca Formation has been interpreted as an open marine setting due to the foraminiferal assemblages overlying it (Timofeeff et al., 2006). The Cretaceous samples from ODP site 627B were deposited on a shallow-water carbonate platform (Austin et al., 1986) that may have been susceptible to non-marine Ca input, but the values and small variability in $\delta^{44/40}Ca$ of gypsum is entirely consistent with the fractionation of gypsum from seawater and a negligible Rayleigh enrichment, rather than non-marine Ca which could push $\delta^{44/40}Ca$ values lighter by up to 1‰. The Messinian samples show some non-marine influence in $^{87}Sr/^{86}Sr$ of the upper evaporite sequence (Hensley, 2006; Müller and Mueller, 1991), which was sampled in ODP site 654A, but the major sources of non-marine Ca are all isotopically light and thus the existence of enriched $\delta^{44/40}Ca$ values in this and other cores of Messinian age is still diagnostic of $SO_4 > Ca$ in seawater. The conclusions from these data are that all the samples in this study faithfully reflect marine major-ion composition.

LOCATION INFORMATION

Silurian	JEM Petroleum 3-7 Bruggers core: 44.488°N, 85.084°W
Permian	Union Oil 37-4 Univ core: 31.781°N, 103.303°W
Cretaceous	Vale Potássio Nordeste core: near Aracaju, at 10.917°S, 37.050°W
	ODP site 627B: 27.635°N, 78.294°W
Messinian	ODP site 654A: 40.579°N, 10.697°E
	ODP site 374Z: 35.848°N, 18.196°E
	ODP site 372Z: 40.031°N, 04.797°E
	ODP site 376Z: 34.872°N, 31.808°E
	ODP site 134Z: 39.200°N, 07.336°E
	ODP site 124Z: 38.873°N, 04.995°E

SUPPLEMENTAL FIGURE CAPTIONS

Figure DR1. Comparison of reconstructed seawater $\delta^{44/40}$Ca from carbonate fossils and barite (Blättler et al., 2012; Farkaš et al., 2007) with that from evaporites, using an offset of 1‰ for the minimum evaporite values measured. The vertical dashed line is the value of modern seawater.

Figure DR2. Theoretical calculations for Rayleigh fractionation of Ca during evaporite precipitation. Black arrows show the range in $\delta^{44/40}$Ca expected in gypsum/anhydrite minerals within the sulfate facies for Ca-rich and SO_4-rich seawaters.

Figure DR3. Ca-isotope data from core Duval C-260, an alternate section of the Permian Castile Formation. This core of homogenous laminated anhydrite/dolomite does not include a lower carbonate facies and does not reach the halite facies, and $\delta^{44/40}$Ca values remain within a very narrow range. This demonstrates the importance of obtaining an evaporite sequence with successions of evaporitic facies for capturing the full range of Ca-isotope variation. The most negative points are considered outliers, due to the lack of a smooth trend with neighboring evaporitic samples, but are possibly indicative of the influence of non-marine Ca in the basin.

REFERENCES CITED

Austin, J.A., Jr., Schlager, W., and Palmer, A.A., 1986, Site 627: Southern Blake Plateau: Proceedings of the Ocean Drilling Program, Initial Reports (Part A), v. 101, p. 111.

Blättler, C.L., Henderson, G.M., and Jenkyns, H.C., 2012, Explaining the Phanerozoic Ca isotope history of seawater: Geology, v. 40, no. 9, p. 843–846.

Brennan, S.T., and Lowenstein, T.K., 2002, The major-ion composition of Silurian seawater: Geochimica et Cosmochimica Acta, v. 66, no. 15, p. 2683–2700.

Brookins, D.G., 1988, Seawater $^{87}Sr/^{86}Sr$ for the Late Permian Delaware Basin evaporites (New Mexico, USA): Chemical Geology, v. 69, no. 3, p. 209–214.

Das, N., Horita, J., and Holland, H.D., 1990, Chemistry of fluid inclusions in halite from the Salina Group of the Michigan basin: Implications for Late Silurian seawater and the origin of sedimentary brines: Geochimica et Cosmochimica Acta, v. 54, no. 2, p. 319–327.

Farkaš, J., Böhm, F., Wallmann, K., Blenkinsop, J., Eisenhauer, A., van Geldern, R., Munnecke, A., Voigt, S., and Veizer, J., 2007, Calcium isotope record of Phanerozoic oceans: Implications for chemical evolution of seawater and its causative mechanisms: Geochimica et Cosmochimica Acta, v. 71, no. 21, p. 5117–5134.

Hensley, T.M., 2006, Calcium isotopic variation in marine evaporites and carbonates: Applications to Late Miocene Mediterranean brine chemistry and Late Cenozoic calcium cycling in the oceans [PhD thesis]: San Diego, California, University of California, 124 p.

Kester, D.R., Duedall, I.W., Connors, D.N., and Pytkowicz, R.M., 1967, Preparation of artificial seawater: Limnology and Oceanography, v. 12, no. 1, p. 176–179.

Kirkland, D.W., Denison, R.E., and Dean, W.E., 2000, Parent Brine of the Castile Evaporites (Upper Permian), Texas and New Mexico: Journal of Sedimentary Research, v. 70, no. 3, p. 749–761.

Müller, D.W., and Mueller, P.A., 1991, Origin and age of the Mediterranean Messinian evaporites: implications from Sr isotopes: Earth and Planetary Science Letters, v. 107, no. 1, p. 1–12.

Risacher, F., and Clement, A., 2001, A computer program for the simulation of evaporation of natural waters to high concentration: Computers & Geosciences, v. 27, no. 2, p. 191–201.

Timofeeff, M.N., Lowenstein, T.K., da Silva, M.A.M., and Harris, N.B., 2006, Secular variation in the major-ion chemistry of seawater: Evidence from fluid inclusions in Cretaceous halites: Geochimica et Cosmochimica Acta, v. 70, no. 8, p. 1977–1994.

Figure DR1

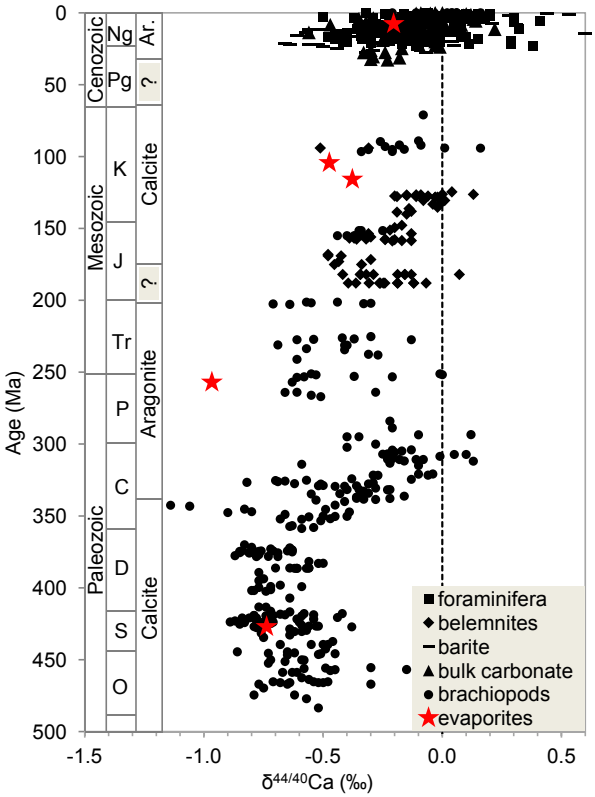
Age (Ma)
0
50
100
150
200
250
300
350
400
450
500
Cenozoic
Mesozoic
Paleozoic
Ng
Pg
K
J
Tr
P
C
D
S
O
Ar.
?
Calcite
?
Aragonite
Calcite
-1.5
-1.0
-0.5
0.0
0.5
δ44/40Ca (‰)
foraminifera
belemnites
barite
bulk carbonate
brachiopods
evaporites

Figure DR2

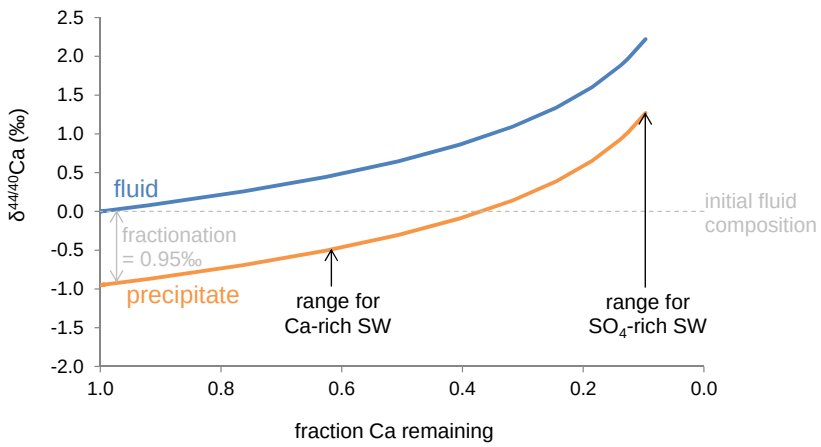
2.5
2.0
1.5
1.0
0.5
0.0
-0.5
-1.0
-1.5
-2.0
δ44/40Ca (‰)
fluid
fractionation
= 0.95‰
precipitate
initial fluid
composition
range for
Ca-rich SW
range for
SO4-rich SW
1.0
0.8
0.6
0.4
0.2
0.0
fraction Ca remaining

Figure DR3

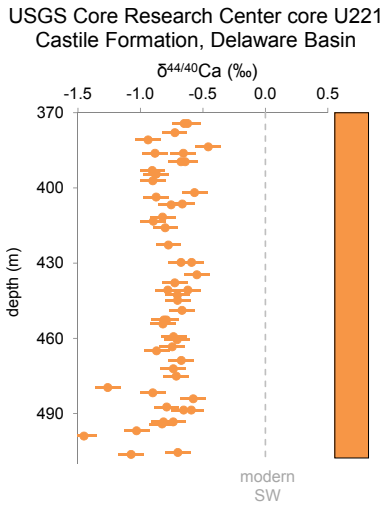
USGS Core Research Center core U221
Castile Formation, Delaware Basin
δ44/40Ca (‰)
-1.5
-1.0
-0.5
0.0
0.5
370
400
430
460
490
depth (m)
modern
SW

Table DR1. Experiment data

sample name	sample type	time (days)	$\delta^{44/42}$Ca relative to internal standard	$\delta^{44/40}$Ca relative to modern seawater	f_Ca (fraction Ca remaining)
artSW	initial fluid	0	0.11	-0.70	1.00
SO_4-rich experiment					
M2-0	fluid	0	0.24	-0.44	1.00
M2-7	fluid	7	0.14	-0.65	0.86
M2-10	fluid	10	0.16	-0.61	0.86
M2-12	fluid	12	0.40	-0.11	0.51
M2-12_2	fluid	12	0.30	-0.31	0.51
M2-14	fluid	14	0.58	0.25	0.44
M2-14_2	fluid	14	0.60	0.29	0.44
M2-15	fluid	15	0.69	0.46	0.37
M2-15_2	fluid	15	0.73	0.53	0.37
M2-16	fluid	16	0.75	0.58	0.24
M2-17	fluid	17	0.99	1.06	0.17
M2-18	fluid	18	1.33	1.74	0.11
M2-19	fluid	19	1.40	1.89	0.01
M2-20	fluid	20	1.43	1.93	0.01
M2-12-c	precipitate	12	-0.25	-1.43	0.51
M2-14-c	precipitate	14	-0.23	-1.37	0.44
M2-15-c	precipitate	15	-0.02	-0.95	0.37
M2-15-c_2	precipitate	15	-0.16	-1.23	0.37
M2-18-c	precipitate	18	0.26	-0.39	0.11
M2-19-c	precipitate	19	0.18	-0.55	0.01
Ca-rich experiment					
S2-0	fluid	0	0.16	-0.59	1.00
S2-7	fluid	7	0.15	-0.62	1.05
S2-10	fluid	10	0.18	-0.55	0.93
S2-12	fluid	12	0.19	-0.54	0.87
S2-14	fluid	14	0.23	-0.46	0.81
S2-15	fluid	15	0.23	-0.46	0.79
S2-16	fluid	16	0.24	-0.45	0.76
S2-16_2	fluid	16	0.19	-0.54	0.76
S2-17	fluid	17	0.26	-0.40	0.74
S2-17_2	fluid	17	0.17	-0.59	0.74
S2-18	fluid	18	0.23	-0.47	0.74
S2-19	fluid	19	0.23	-0.46	0.73
S2-20	fluid	20	0.26	-0.40	0.73
S2-11-c	precipitate	11	-0.36	-1.63	0.90
S2-11-c_2	precipitate	11	-0.31	-1.54	0.90
S2-11.5-c	precipitate	11	-0.36	-1.63	0.90
S2-12-c	precipitate	12	-0.31	-1.55	0.87
S2-14-c	precipitate	14	-0.31	-1.54	0.81
S2-15-c	precipitate	15	-0.33	-1.59	0.79
S2-15-c_2	precipitate	15	-0.17	-1.26	0.79

S2-18-c	precipitate	18	-0.19	-1.30	0.74
S2-18-c_2	precipitate	18	-0.25	-1.43	0.74
S2-18-c_3	precipitate	18	-0.09	-1.10	0.74
S2-19-c	precipitate	19	-0.04	-1.00	0.73
S2-19-c_2	precipitate	19	-0.08	-1.09	0.73

Table DR2. Messinian data

sample name	sample type	relative depth (m) within recovered core	$\delta^{44/42}$Ca relative to internal standard	$\delta^{44/40}$Ca relative to modern seawater
654A-28R-1W-4-5	gypsum	0.04	-0.06	-1.05
654A-28R-1W-4-5_2	gypsum	0.04	-0.06	-1.03
654A-28R-1W-33-34	gypsum	0.33	-0.06	-1.04
654A-28R-1W-62-63	gypsum	0.62	-0.12	-1.17
654A-30R-1W-70-72	gypsum	9.20	0.18	-0.56
654A-30R-1W-91-92	gypsum	9.41	-0.07	-1.06
654A-30R-1W-33-34	calcite	8.83	0.01	-0.89
654A-30R-1W-121-122	gypsum	9.71	-0.10	-1.12
654A-30R-1W-135-136	gypsum	9.85	-0.07	-1.06
654A-31R-1W-107-108	gypsum	11.07	-0.12	-1.16
654A-31R-1W-121-122	gypsum	11.21	0.08	-0.76
654A-31R-1W-144-145	gypsum	11.44	0.04	-0.83
654A-34R-1A-19-20	gypsum	16.29	0.08	-0.75
654A-34R-1A-47-48	gypsum	16.57	0.16	-0.59
654A-34R-1A-76-76.5	gypsum	16.86	0.18	-0.57
654A-34R-1A-107-108	gypsum	17.17	0.22	-0.48
654A-34R-1A-136-138	gypsum	17.46	0.17	-0.59
654A-34R-2W-2-3	gypsum	17.62	0.20	-0.51
654A-34R-2W-31-32	gypsum	17.91	0.09	-0.73
654A-34R-2W-64-65	gypsum	18.24	0.13	-0.66
654A-34R-2W-92-93	gypsum	18.52	0.12	-0.68
654A-34R-2W-122-123	gypsum	18.82	0.07	-0.79
654A-34R-2W-145-146	gypsum	19.05	-0.04	-1.00
654A-34R-3W-2-3	gypsum	19.12	0.18	-0.57
654A-34R-3W-2-3_2	gypsum	19.12	0.08	-0.77
654A-34R-3W-28-29	gypsum	19.38	0.08	-0.76
654A-34R-3W-63-64	gypsum	19.73	0.04	-0.83
654A-34R-3W-90-91	gypsum	20.00	0.16	-0.60
654A-34R-3W-123-124	gypsum	20.33	0.05	-0.82
654A-34R-3W-146-147	gypsum	20.56	0.10	-0.71
654A-36R-1W-44-45	gypsum	23.94	0.48	0.04
654A-36R-1W-83-84	gypsum	24.33	0.51	0.11
654A-36R-1W-83-84_2	gypsum	24.33	0.36	-0.20
654A-36R-1W-110-110.5	gypsum	24.60	0.41	-0.09
654A-36R-1W-144-145	calcite	24.94	0.18	-0.56
374Z-18R-1W-127-128	gypsum/anhydrite	1.27	0.34	-0.24
374Z-18R-1W-136-137	gypsum	1.36	0.37	-0.18
374Z-19R-1W-89-90	gypsum/anhydrite	1.39	0.37	-0.18
374Z-19R-1W-89-90_2	gypsum/anhydrite	1.39	0.58	0.24
374Z-19R-1W-131-132	gypsum/anhydrite	1.81	0.24	-0.44
374Z-21R-1W-117-118	anhydrite	4.37	0.21	-0.51
374Z-21R-1W-132-133	anhydrite	4.52	0.34	-0.24
374Z-21R-1W-138-139	anhydrite	4.58	0.33	-0.26
374Z-21R-1W-144-145	anhydrite	4.64	0.25	-0.42
374Z-22R-1A-110-111	gypsum	4.80	0.23	-0.46
372Z-8R-1W-57-58	gypsum	0.57	0.18	-0.56
372Z-8R-1W-86-87	gypsum	0.86	0.18	-0.56
372Z-8R-1W-115-116	gypsum	1.15	0.22	-0.48
372Z-8R-2W-146-147	gypsum	1.46	0.03	-0.86
376Z-22R-1A-40-50	gypsum	0.40	0.52	0.12

376Z-22R-1A-86-87	gypsum	0.86	0.43	-0.06
376Z-22R-1A-118-119	gypsum	1.18	0.48	0.03
376Z-22R-1A-131-132	anhydrite	1.31	0.45	-0.02
376Z-22R-1A-136-140	gypsum/anhydrite	1.36	0.46	-0.01
134Z-10R-1W-79-80	anhydrite	0.00	0.07	-0.79
124Z-8R-1W-30-31	anhydrite	0.30	0.15	-0.61
124Z-8R-1W-92-93	anhydrite	0.92	0.31	-0.31
124Z-8R-1W-124-125	anhydrite	1.24	0.16	-0.61

Table DR3. Cretaceous data

sample name	sample type	relative depth (m) within recovered core	$\delta^{44/42}$Ca relative to internal standard	$\delta^{44/40}$Ca relative to modern seawater
627B-55X-1W-3-5	gypsum	0.03	-0.20	-1.33
627B-55X-1W-3-5_2	gypsum	0.03	-0.21	-1.34
627B-55X-1W-14-15	gypsum	0.14	-0.22	-1.36
627B-55X-1W-22-24	gypsum	0.22	-0.23	-1.38
627B-55X-1W-22-24_2	gypsum	0.22	-0.25	-1.43
627B-55X-1W-30-32	gypsum	0.30	-0.20	-1.33
627B-55X-1W-30-32_2	gypsum	0.30	-0.22	-1.37
627B-55X-1W-44-45	gypsum	0.44	-0.21	-1.34
627B-55X-1W-50-51	gypsum	0.50	-0.26	-1.44
627B-55X-1W-66-67	gypsum	0.66	-0.21	-1.33
627B-55X-1W-66-67_2	gypsum	0.66	-0.21	-1.34
627B-55X-1W-74-75	gypsum	0.74	-0.16	-1.24
627B-55X-1W-74-75_2	gypsum	0.74	-0.24	-1.39
627B-55X-1W-80-81	gypsum	0.80	-0.28	-1.48
627B-55X-1W-92-93	gypsum	0.92	-0.20	-1.33
627B-55X-1W-92-93_2	gypsum	0.92	-0.19	-1.30
627B-55X-1W-102-103	gypsum	1.02	-0.16	-1.24
627B-56X-1W-18-20	gypsum	2.07	-0.21	-1.34
627B-56X-1W-31-32	gypsum	2.20	-0.17	-1.26
627B-56X-CCW-8-9	gypsum	2.37	-0.21	-1.34
627B-59X-1W-1-2	gypsum	5.93	-0.23	-1.38
627B-59X-1W-11-12	gypsum	6.03	-0.21	-1.35
627B-59X-1W-21-22	gypsum	6.13	-0.23	-1.38
627B-59X-1W-34-35	gypsum	6.26	-0.12	-1.16
627B-59X-1W-34-35_2	gypsum	6.26	-0.18	-1.28
627B-59X-1W-40-43	gypsum	6.32	-0.11	-1.15
627B-59X-1W-40-43_2	gypsum	6.32	-0.26	-1.44
627B-59X-1W-51-52	gypsum	6.43	-0.12	-1.17
627B-60X-1W-0-2	gypsum	6.98	-0.07	-1.07
627B-60X-1W-13-14	gypsum	7.11	-0.11	-1.13
627B-60X-1W-13-14_2	gypsum	7.11	-0.18	-1.28
627B-60X-1W-35-36	gypsum	7.33	-0.23	-1.37

627B-60X-CCW-16-17	gypsum	7.64	-0.14	-1.19
627B-60X-CCW-16-17_2	gypsum	7.64	-0.18	-1.29

sample name	sample type	depth (m)	$\delta^{44/42}$Ca relative to internal standard	$\delta^{44/40}$Ca relative to modern seawater
Vale-301.25	anhydrite	301.25	-0.05	-1.02
Vale-301.25-B	anhydrite	301.25	-0.13	-1.18
Vale-301.35	anhydrite	301.35	-0.18	-1.29
Vale-301.55	anhydrite	301.55	-0.08	-1.08
Vale-301.55-B	anhydrite	301.55	-0.09	-1.09
Vale-306.45	anhydrite	306.45	-0.22	-1.36
Vale-306.45-B	anhydrite	306.45	-0.22	-1.37
Vale-306.45-C	anhydrite	306.45	-0.15	-1.22
Vale-306.5	anhydrite	306.50	-0.20	-1.32
Vale-306.6	anhydrite	306.60	-0.20	-1.31
Vale-308.2	anhydrite	308.20	-0.21	-1.34
Vale-308.2-B	anhydrite	308.20	-0.21	-1.34
Vale-308.7	anhydrite	308.70	-0.11	-1.14
Vale-308.7-B	anhydrite	308.70	-0.14	-1.19
Vale-310.05	anhydrite	310.05	-0.16	-1.24
Vale-321.8	anhydrite	321.80	-0.11	-1.14
Vale-322.5	anhydrite	322.50	-0.13	-1.17

Table DR4. Permian data

sample name	sample type	depth (m)	$\delta^{44/42}$Ca relative to internal standard	$\delta^{44/40}$Ca relative to modern seawater
E420-3972.5	anhydrite	1210.8	0.19	-0.55
E420-3973.4	anhydrite	1211.1	0.16	-0.61
E420-3976.1	anhydrite	1211.9	0.08	-0.75
E420-3979.6	anhydrite	1213.0	0.07	-0.77
E420-3990	anhydrite	1216.2	0.13	-0.66
E420-4000	anhydrite	1219.2	0.09	-0.73
E420-4010	anhydrite	1222.2	-0.01	-0.93
E420-4020	anhydrite	1225.3	-0.03	-0.98
E420-4030	anhydrite	1228.3	0.04	-0.84
E420-4040	anhydrite	1231.4	0.15	-0.62
E420-4050	anhydrite	1234.4	0.15	-0.63
E420-4060	anhydrite	1237.5	0.16	-0.59
E420-4070	anhydrite	1240.5	0.09	-0.74
E420-4080	anhydrite	1243.6	0.14	-0.65
E420-4090	anhydrite	1246.6	0.10	-0.72
E420-4100	anhydrite	1249.7	0.13	-0.66
E420-4110	anhydrite	1252.7	0.13	-0.65
E420-4120.2	anhydrite	1255.8	0.14	-0.64
E420-4130.2	anhydrite	1258.9	0.11	-0.71
E420-4140	anhydrite	1261.9	0.15	-0.62
E420-4150	anhydrite	1264.9	0.23	-0.47
E420-4150_2	anhydrite	1264.9	0.27	-0.39
E420-4160	anhydrite	1268.0	0.17	-0.57
E420-4170	anhydrite	1271.0	0.23	-0.46
E420-4179.9	anhydrite	1274.0	0.12	-0.68
E420-4190	anhydrite	1277.1	0.11	-0.69
E420-4200	anhydrite	1280.2	0.15	-0.62
E420-4210	anhydrite	1283.2	0.21	-0.50
E420-4220	anhydrite	1286.3	0.12	-0.68
E420-4230	anhydrite	1289.3	0.05	-0.81
E420-4240	anhydrite	1292.4	0.10	-0.72
E420-4250	anhydrite	1295.4	0.14	-0.65
E420-4260	anhydrite	1298.4	0.09	-0.73
E420-4269	anhydrite	1301.2	0.14	-0.65
E420-4280	anhydrite	1304.5	0.19	-0.53
E420-4288.8	anhydrite	1307.2	0.31	-0.29
E420-4404	anhydrite	1342.3	0.26	-0.41
E420-4404.5	anhydrite	1342.5	0.28	-0.36
E420-4406	anhydrite	1342.9	0.15	-0.62
E420-4408	anhydrite	1343.6	0.22	-0.48
E420-4414	anhydrite	1345.4	0.11	-0.71
E420-4422	anhydrite	1347.8	0.09	-0.74
E420-4430	anhydrite	1350.3	0.06	-0.79

E420-4438	anhydrite	1352.7	0.10	-0.72
E420-4446	anhydrite	1355.1	0.09	-0.74
E420-4454	anhydrite	1357.6	0.12	-0.69
E420-4462	anhydrite	1360.0	0.19	-0.53
E420-4470	anhydrite	1362.5	0.12	-0.69
E420-4478	anhydrite	1364.9	0.15	-0.62
E420-4485.7	anhydrite	1367.2	0.14	-0.63
E420-4485.7_2	anhydrite	1367.2	0.13	-0.73
E420-4494	anhydrite	1369.8	0.08	-0.75
E420-4502	anhydrite	1372.2	-0.02	-0.96
E420-4510.1	anhydrite	1374.7	0.00	-0.93
E420-4517.0	anhydrite	1376.8	0.18	-0.56
E420-4517.1	anhydrite	1376.8	0.26	-0.40
E420-4658.3	anhydrite	1419.8	0.26	-0.40
E420-4659.8	anhydrite	1420.3	0.23	-0.45
E420-4660.7	anhydrite	1420.6	0.12	-0.68
E420-4660.7_2	anhydrite	1420.6	0.26	-0.49
E420-4665	anhydrite	1421.9	0.24	-0.43
E420-4670	anhydrite/dolomite	1423.4	0.14	-0.63
E420-4675	anhydrite/dolomite	1424.9	0.09	-0.75
E420-4675_2	anhydrite	1424.9	0.25	-0.51
E420-4680	anhydrite	1426.5	0.19	-0.55
E420-4685	anhydrite	1428.0	0.07	-0.77
E420-4685_2	anhydrite	1428.0	0.21	-0.58
E420-4690	anhydrite	1429.5	0.17	-0.58
E420-4695	anhydrite	1431.0	0.11	-0.69
E420-4700	anhydrite	1432.6	0.14	-0.63
E420-4705	anhydrite	1434.1	0.10	-0.72
E420-4705_2	anhydrite	1434.1	0.18	-0.65
E420-4710	anhydrite	1435.6	0.15	-0.61
E420-4715	anhydrite	1437.1	0.04	-0.84
E420-4715_2	anhydrite	1437.1	0.10	-0.80
E420-4720	anhydrite	1438.7	0.14	-0.64
E420-4725	anhydrite	1440.2	0.11	-0.71
E420-4730	anhydrite	1441.7	0.15	-0.61
E420-4734	anhydrite	1442.9	-0.01	-0.94
E420-4734_2	anhydrite	1442.9	0.18	-0.65
E420-4940	anhydrite/calcite	1505.7	-0.10	-1.12
E420-4940_2	anhydrite/calcite	1505.7	0.03	-0.95
E420-4945	anhydrite	1507.2	-0.04	-1.00
E420-4945_2	anhydrite	1507.2	0.02	-0.97
E420-4955	anhydrite	1510.3	0.00	-0.92
E420-4955_2	anhydrite	1510.3	0.09	-0.83
E420-4965	anhydrite	1513.3	0.07	-0.79
E420-4975	anhydrite	1516.4	-0.07	-1.05
E420-4975_2	anhydrite	1516.4	0.08	-0.84
E420-4983	anhydrite/calcite	1518.8	-0.30	-1.52
E420-4983_2	anhydrite/calcite	1518.8	-0.25	-1.50

E420-4985	anhydrite/calcite	1519.4	-0.03	-0.98
E420-4985_2	anhydrite/calcite	1519.4	0.07	-0.85
E420-4995	calcite	1522.5	-0.52	-1.97
E420-4995_2	calcite	1522.5	-0.39	-1.79
E420-5005	calcite	1525.5	-0.40	-1.72
E420-5005_2	calcite	1525.5	-0.29	-1.59
E420-5015	calcite	1528.6	-0.38	-1.68

Table DR5. Silurian data

sample name	sample type	depth (m)	$\delta^{44/42}$Ca relative to internal standard	$\delta^{44/40}$Ca relative to modern seawater
8090-1	dolomite	2465.86	-0.36	-1.63
8090-8_1	dolomite	2466.08	-0.22	-1.35
8090-8_2	dolomite	2466.08	-0.22	-1.36
8090-8_3	dolomite	2466.08	-0.32	-1.56
8090-8_4	dolomite	2466.08	-0.27	-1.46
8392-3_1	anhydrite	2557.97	-0.25	-1.41
8392-3_2	anhydrite	2557.98	-0.36	-1.64
8392-3_2_2	anhydrite	2557.99	-0.40	-1.72
8392-3_3	anhydrite	2558.00	-0.38	-1.68
8392-3_4	anhydrite	2558.01	-0.36	-1.64
8392-3_5	anhydrite	2558.02	-0.28	-1.48
8392-3_6	anhydrite	2558.03	-0.20	-1.31
8392-3_7	anhydrite	2558.04	-0.22	-1.36
8396-3_1	anhydrite	2559.19	-0.33	-1.59
8396-3_2	anhydrite	2559.19	-0.31	-1.55
8396-3_3	anhydrite	2559.19	-0.19	-1.30
8399-8_1	anhydrite	2560.26	-0.32	-1.56
8399-8_2	anhydrite	2560.26	-0.40	-1.72
8399-8_3	anhydrite	2560.26	-0.39	-1.70
8399-8_4	anhydrite	2560.26	-0.25	-1.42
8402-8_1	anhydrite	2561.17	-0.39	-1.70
8402-8_2	anhydrite	2561.17	-0.37	-1.67
8402-8_3	anhydrite	2561.17	-0.30	-1.51
8402-8_4	anhydrite	2561.17	-0.39	-1.70
8402-8_5	anhydrite	2561.17	-0.35	-1.62
8403-3_1	anhydrite	2561.33	-0.23	-1.38
8403-3_3	anhydrite	2561.34	-0.25	-1.42
8403-3_5	anhydrite	2561.35	-0.31	-1.55
8403-3_7	anhydrite	2561.36	-0.27	-1.45
8403-3_9	anhydrite	2561.37	-0.29	-1.50
8403-3_11	anhydrite	2561.38	-0.22	-1.36
8403-3_13	anhydrite	2561.39	-0.35	-1.63
8403-3_15	anhydrite	2561.40	-0.33	-1.58
8403-3_17	anhydrite	2561.41	-0.31	-1.55
8407-1_1	anhydrite	2562.48	-0.39	-1.70
8407-1_2	anhydrite	2562.49	-0.35	-1.62

8407-1_3	anhydrite	2562.50	-0.28	-1.48
8407-1_4	anhydrite	2562.51	-0.34	-1.60
8401-1_5	anhydrite	2562.52	-0.32	-1.56

Table DR6. Permian Supp data

sample name	sample type	depth (m)	$\delta^{44/42}$Ca relative to internal standard	$\delta^{44/40}$Ca relative to modern seawater
C1228	anhydrite	374.3	0.15	-0.62
C1228_2	anhydrite	374.3	0.14	-0.65
C1240	anhydrite	378.0	0.10	-0.72
C1249.5	anhydrite	380.8	-0.01	-0.94
C1258.5	anhydrite/dolomite	383.6	0.23	-0.46
C1267	anhydrite	386.2	0.02	-0.88
C1267_2	anhydrite	386.2	0.13	-0.66
C1278	anhydrite	389.5	0.12	-0.67
C1278_2	anhydrite	389.5	0.14	-0.64
C1289.5	anhydrite	393.0	0.01	-0.91
C1294.2	anhydrite	394.5	0.02	-0.88
C1294.2_2	anhydrite	394.5	0.02	-0.87
C1303	anhydrite	397.2	0.01	-0.90
C1318.5	anhydrite	401.9	0.18	-0.57
C1324.3	anhydrite	403.6	0.02	-0.87
C1333.3	anhydrite/dolomite	406.4	0.13	-0.66
C1334.5	anhydrite/dolomite	406.8	0.08	-0.75
C1350.5	anhydrite/dolomite	411.6	0.05	-0.82
C1356	anhydrite	413.3	0.01	-0.90
C1364.5	anhydrite	415.9	0.06	-0.80
C1387	anhydrite/calcite	422.8	0.07	-0.78
C1409.8	anhydrite/calcite	429.7	0.12	-0.67
C1409.8_2	anhydrite	429.7	0.16	-0.59
C1426	anhydrite	434.6	0.19	-0.55
C1436.5	anhydrite	437.8	0.10	-0.72
C1446	anhydrite/dolomite	440.7	0.07	-0.78
C1446_2	anhydrite/dolomite	440.7	0.15	-0.62
C1452.5	anhydrite/dolomite	442.7	0.11	-0.70
C1459.5	anhydrite	444.9	0.11	-0.70
C1472.5	anhydrite	448.8	0.13	-0.67
C1485	anhydrite/calcite	452.6	0.05	-0.81
C1485_2	anhydrite/calcite	452.6	0.06	-0.79
C1490.3	anhydrite/calcite	454.2	0.05	-0.82
C1507	anhydrite/calcite	459.3	0.09	-0.73
C1511	anhydrite/calcite	460.6	0.11	-0.71
C1520.2	anhydrite	463.4	0.09	-0.74
C1525.5	anhydrite	465.0	0.02	-0.87
C1538	anhydrite	468.8	0.12	-0.67
C1549	anhydrite/dolomite	472.1	0.09	-0.74
C1558.5	anhydrite	475.0	0.10	-0.71
C1573.5	calcite/anhydrite	479.6	-0.17	-1.26
C1580.5	anhydrite/dolomite	481.7	0.01	-0.90
C1588.2	anhydrite/dolomite	484.1	0.17	-0.58
C1599	anhydrite/dolomite	487.4	0.07	-0.79

C1603	anhydrite/dolomite	488.6	0.13	-0.65
C1603_2	anhydrite/dolomite	488.6	0.16	-0.59
C1618.5	anhydrite/dolomite	493.3	0.09	-0.74
C1618.5_2	anhydrite/dolomite	493.3	0.05	-0.81
C1621.2	anhydrite	494.1	0.05	-0.83
C1630	anhydrite/dolomite	496.8	-0.06	-1.03
C1637	anhydrite/calcite	499.0	-0.27	-1.45
C1658.5	anhydrite	505.5	0.11	-0.70
C1661	anhydrite/dolomite/calcite/quartz	506.3	-0.08	-1.07